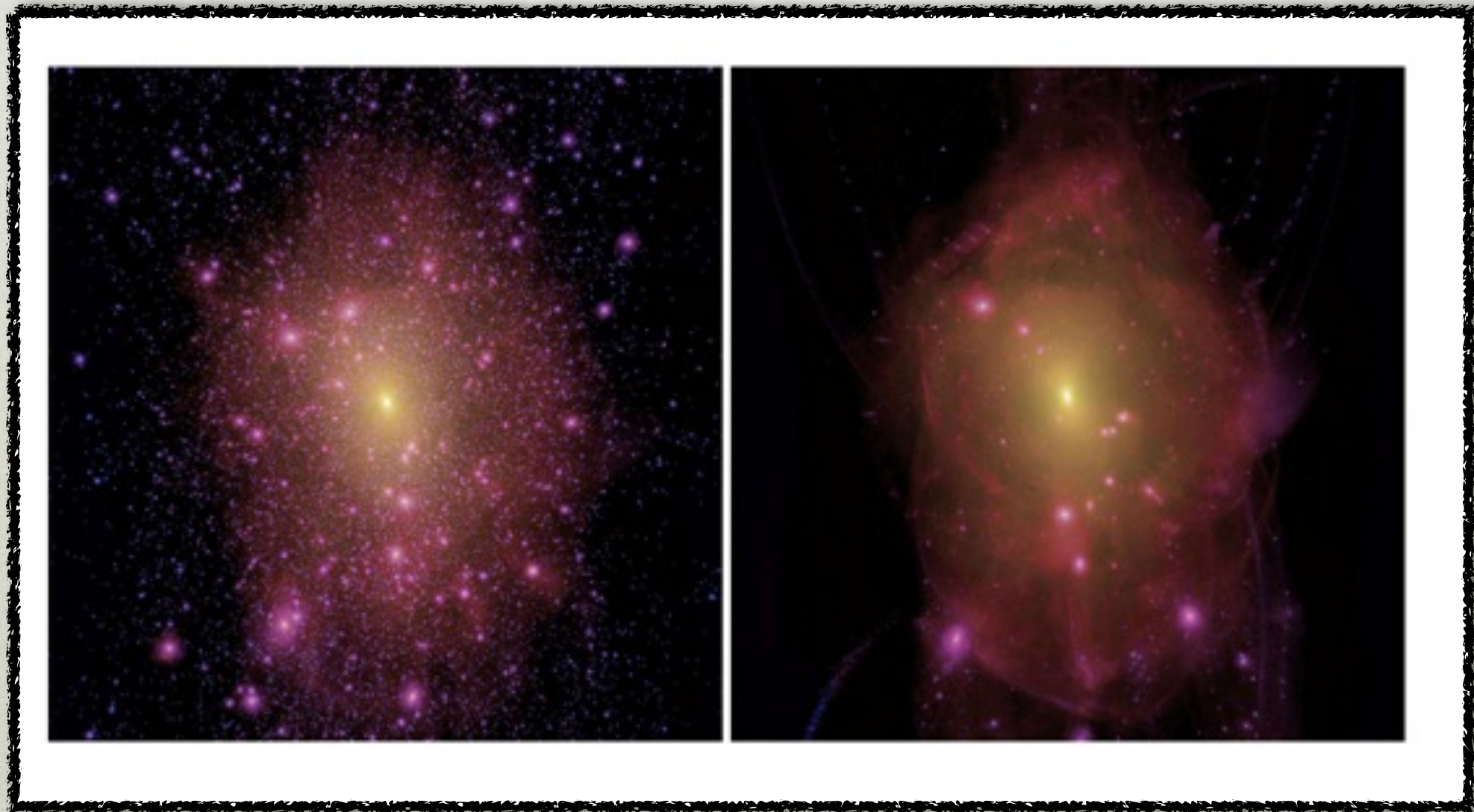


CDM SUBSTRUCTURE MASS FUNCTION AT $z \sim 0.2$



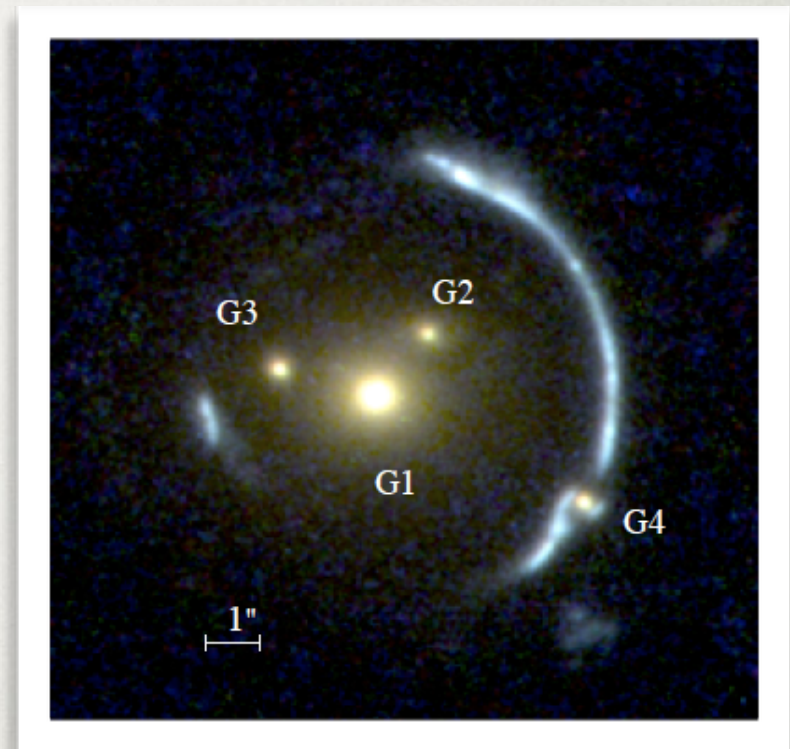
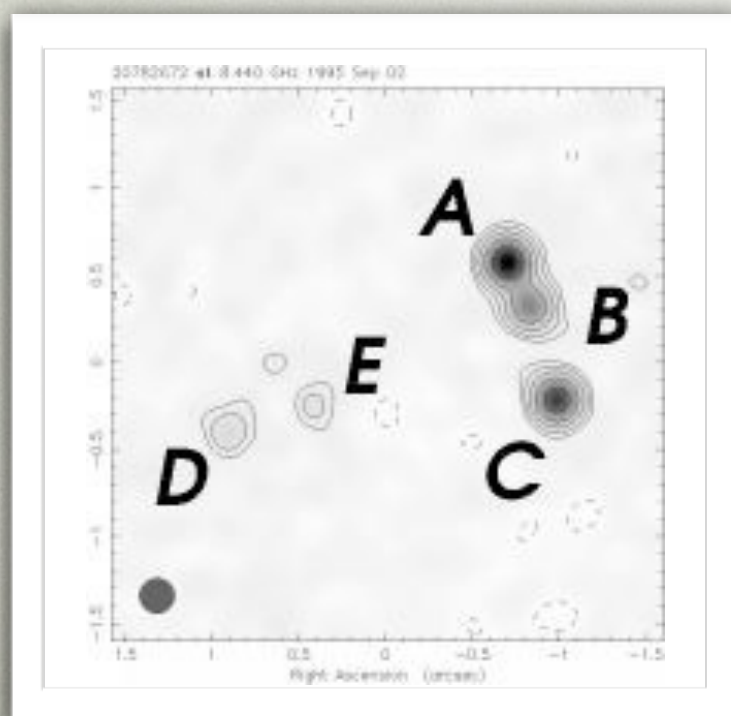
SIMONA VEGETTI - MPA

CDM vs WDM



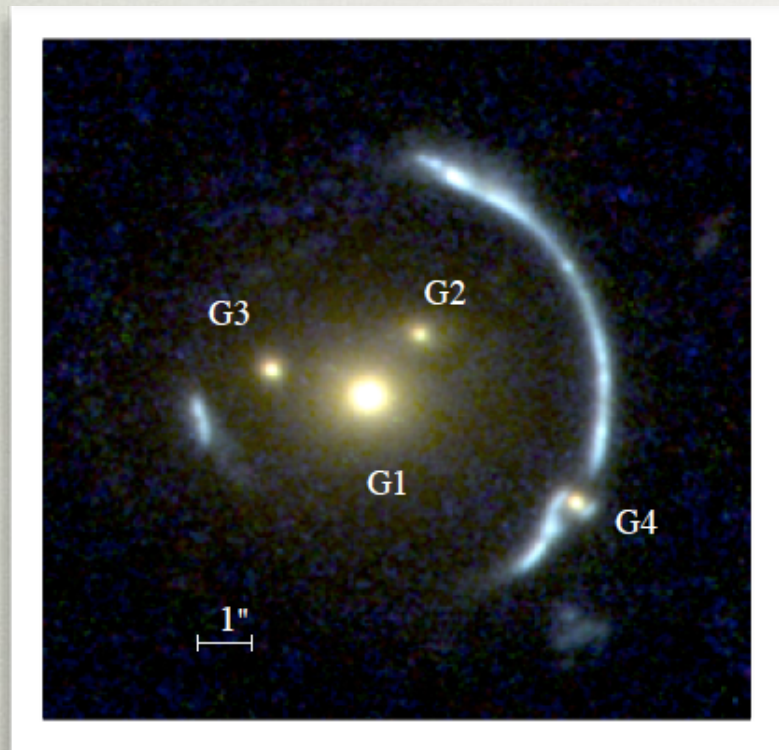
GRAVITATIONAL IMAGING

- [substructures are detected as magnification anomalies
- [Compact sources are easy to model
- [Sensitive to a wide range of masses
- [degenerate in the mass model



- [substructures are detected as surface brightness anomalies
- [need to disentangle structures in the potential from structures in the source
- [Sensitive to higher masses
- [NOT degenerate in the mass model

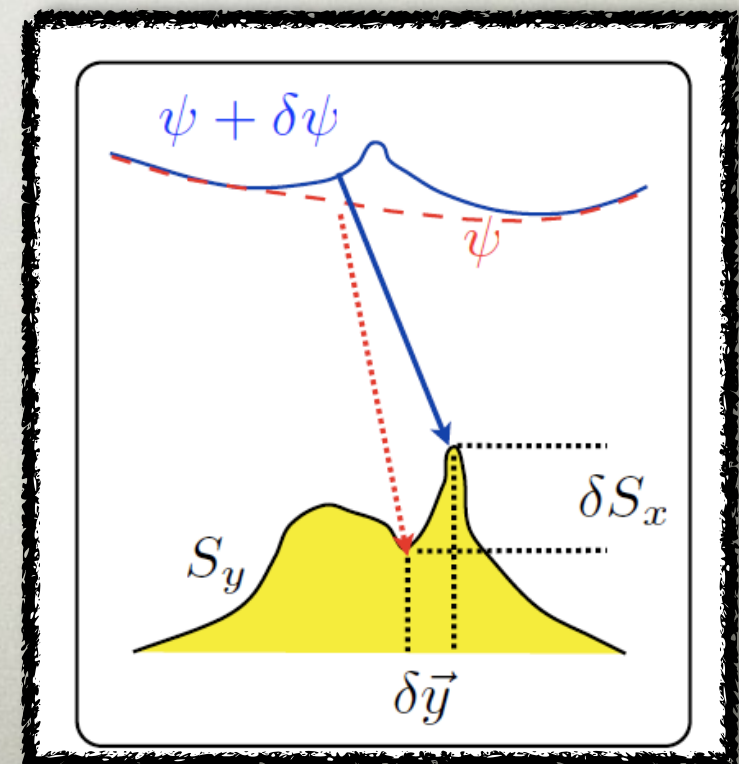
GRAVITATIONAL IMAGING



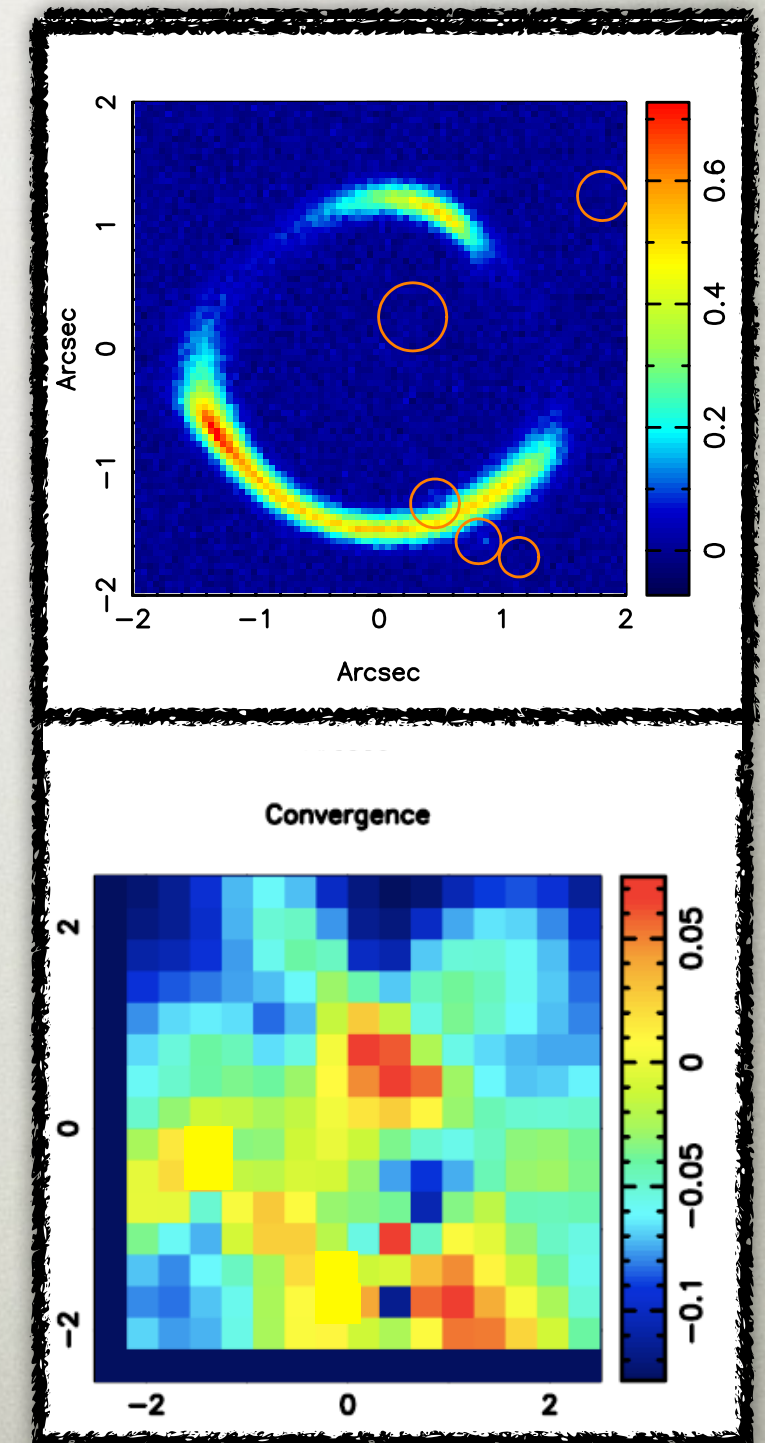
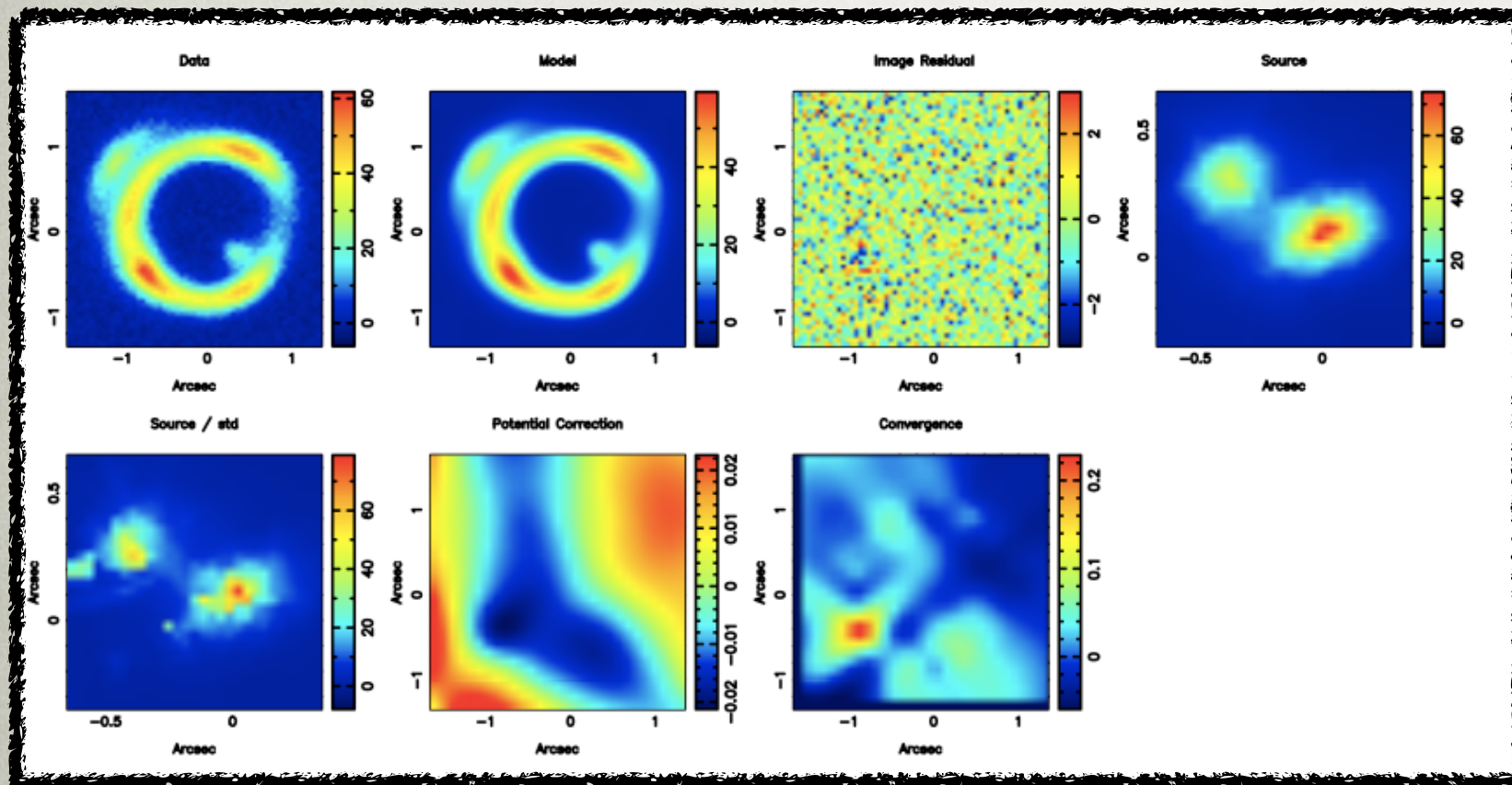
$$\psi(\mathbf{x}, \eta)_{tot} = \psi(\mathbf{x}, \eta) + \delta\psi(\mathbf{x})$$

$\psi(\mathbf{x}, \eta)$ Smooth analytic power-law model

$\delta\psi(\mathbf{x})$ pixellated potential correction



GRAVITATIONAL IMAGING



- substructures are responsible of localised surface brightness perturbations and are detected as localised potential corrections
- Any substructure can be detected provided it is mass enough and / or close enough to the Einstein ring
- For each substructure detected its mass can be measured by assuming a mass model or directly from the pixelated corrections in a model independent way

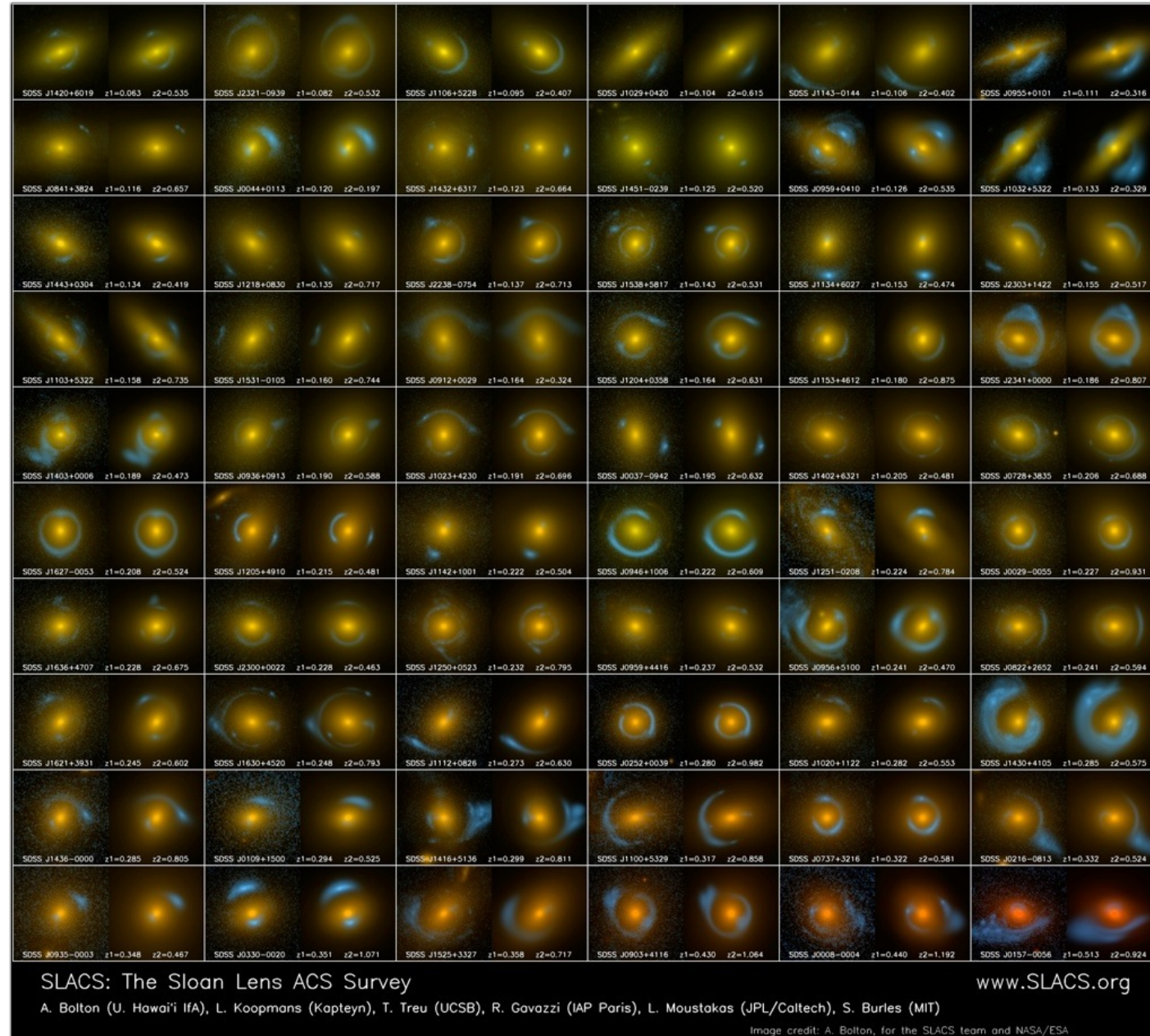
CRITERIA FOR DETECTION

- a positive convergence correction that improves the image residuals is found independently from the potential regularization, number of source pixels, PSF rotations, and galaxy subtraction procedure;
- a clumpy model is preferred over a smooth model with a Bayes factor $\Delta \log E = \log E_{\text{smooth}} - \log E_{\text{clumpy}} \geq -50$ (to first order equivalent to a $10\text{-}\sigma$ detection, under the assumption of Gaussian noise);
- the mass and the position of the substructure obtained via the Nested Sampling analysis is consistent with those independently obtained by the potential corrections and the MAP parametric clumpy model;
- the results are consistent among the different HST filters, where available.

Bolton et al. 2006

Bolton et al. 2008

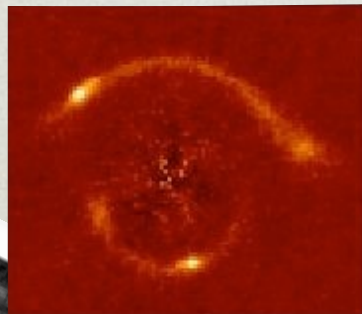
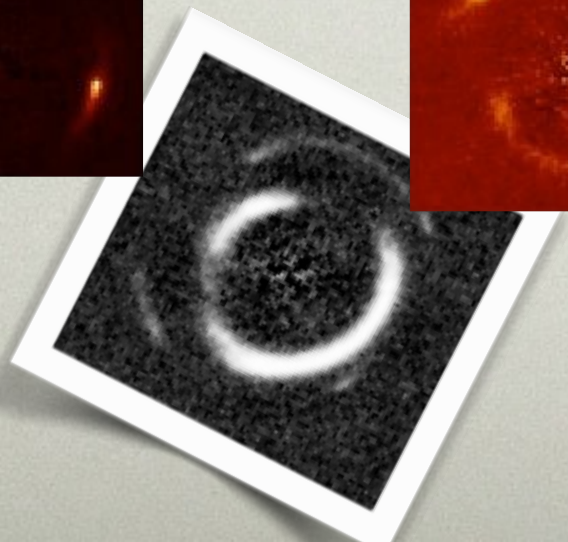
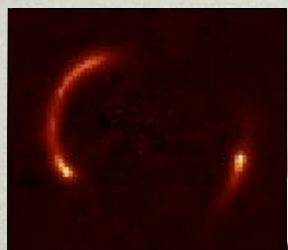
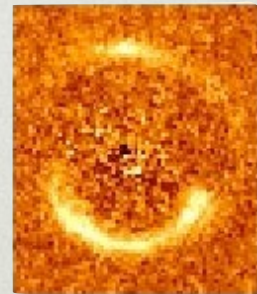
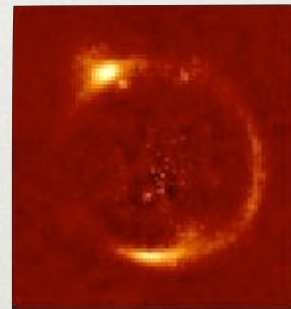
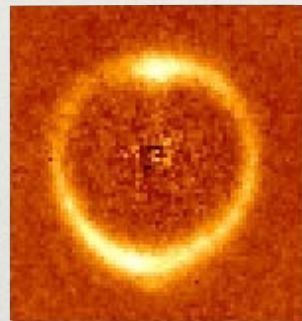
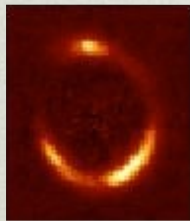
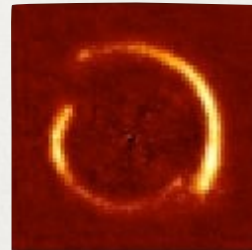
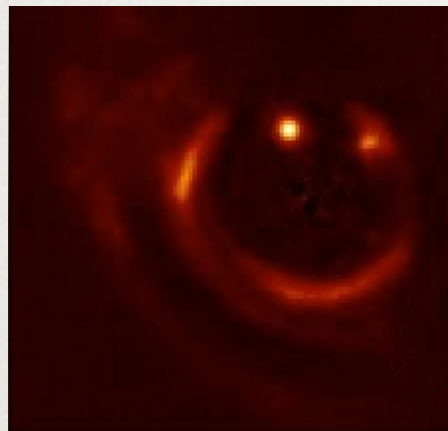
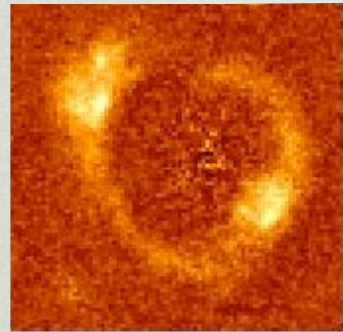
SLACS



$$z = 0.06 - 0.36$$

$$\sigma_{\star} = 175 - 400 \text{ km s}^{-1}$$

$$z = 0.06 - 0.36 \quad \sigma_{\star} = 175 - 400 \text{ km s}^{-1}$$



Chosen on a s/n basis

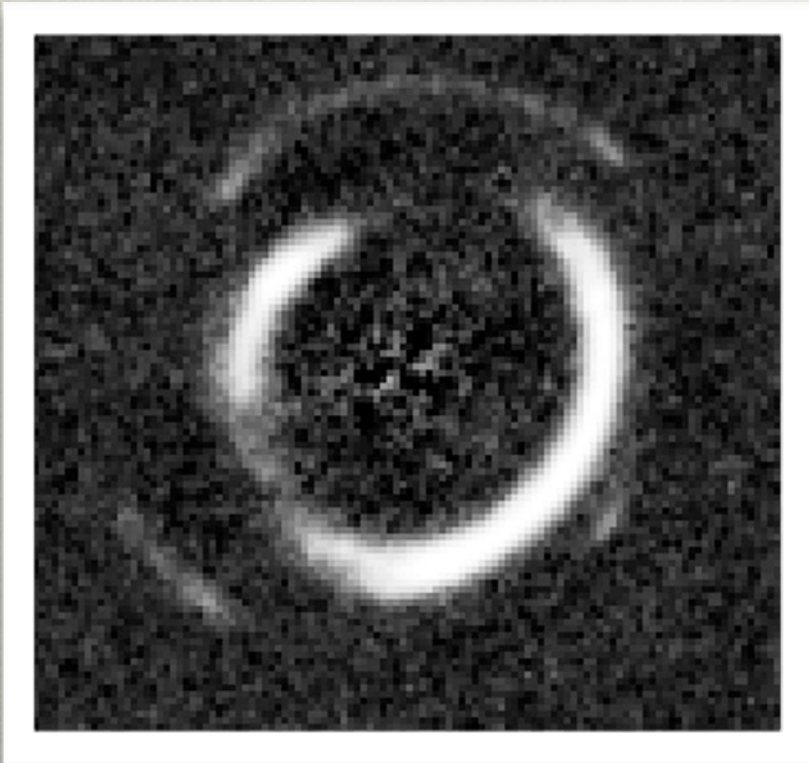


Representative sub-sample of the
SLACS lenses



Representative sample of massive
early-type galaxies

SLACS-DOUBLE RING



→ Two concentric ring-like structures

→ Dark-matter fraction: $f(< R_{eff}) = 73\% \pm 9\%$

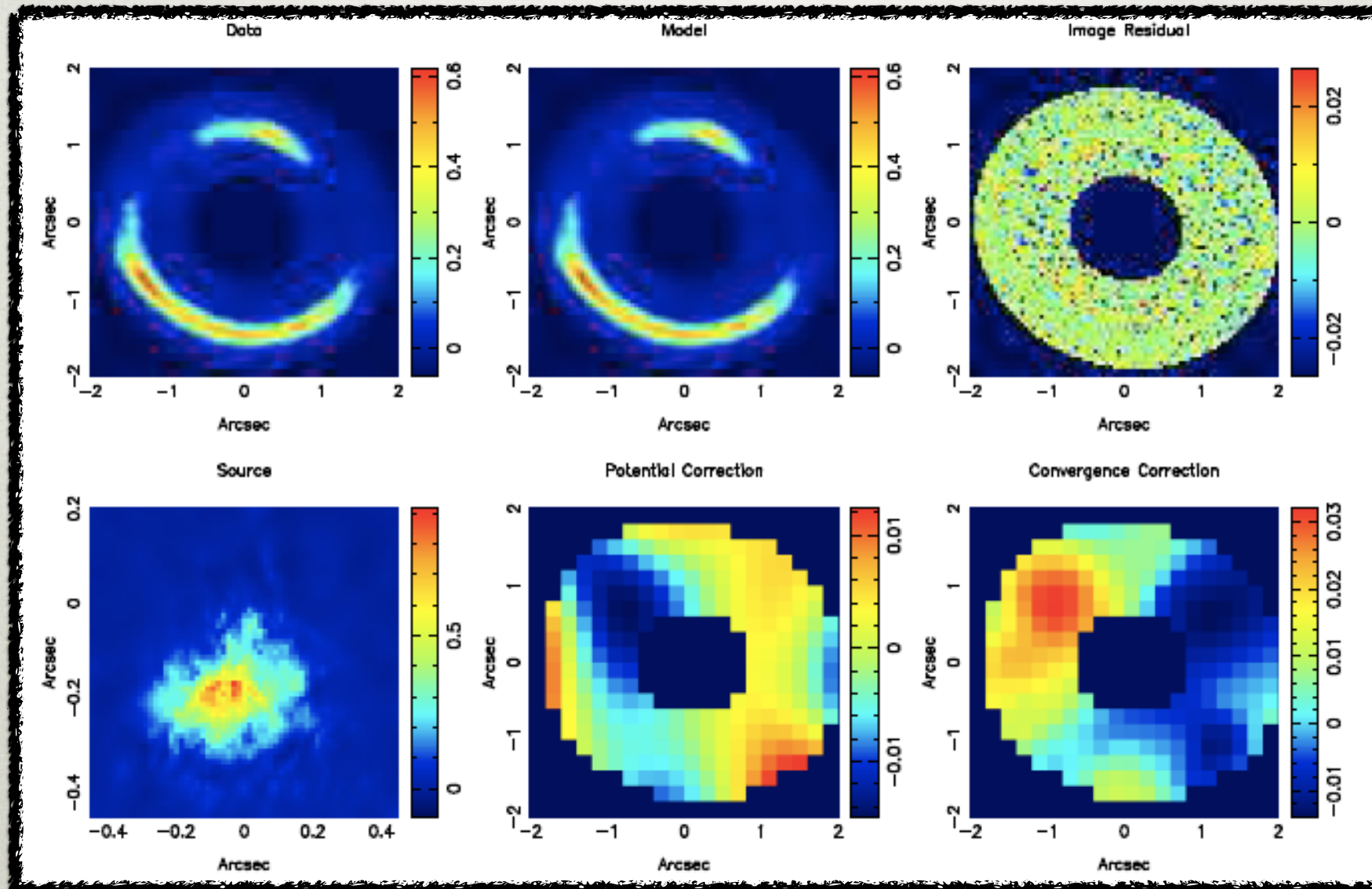
→ Expected number of mass substructure from CDM paradigm within

$$\Delta R = R_{ein} \pm 0.3$$

→ If $f \sim 5\%$ (Dalal & Kochanek 2002), the expectation values for mass substructure is ~ 50 substructures

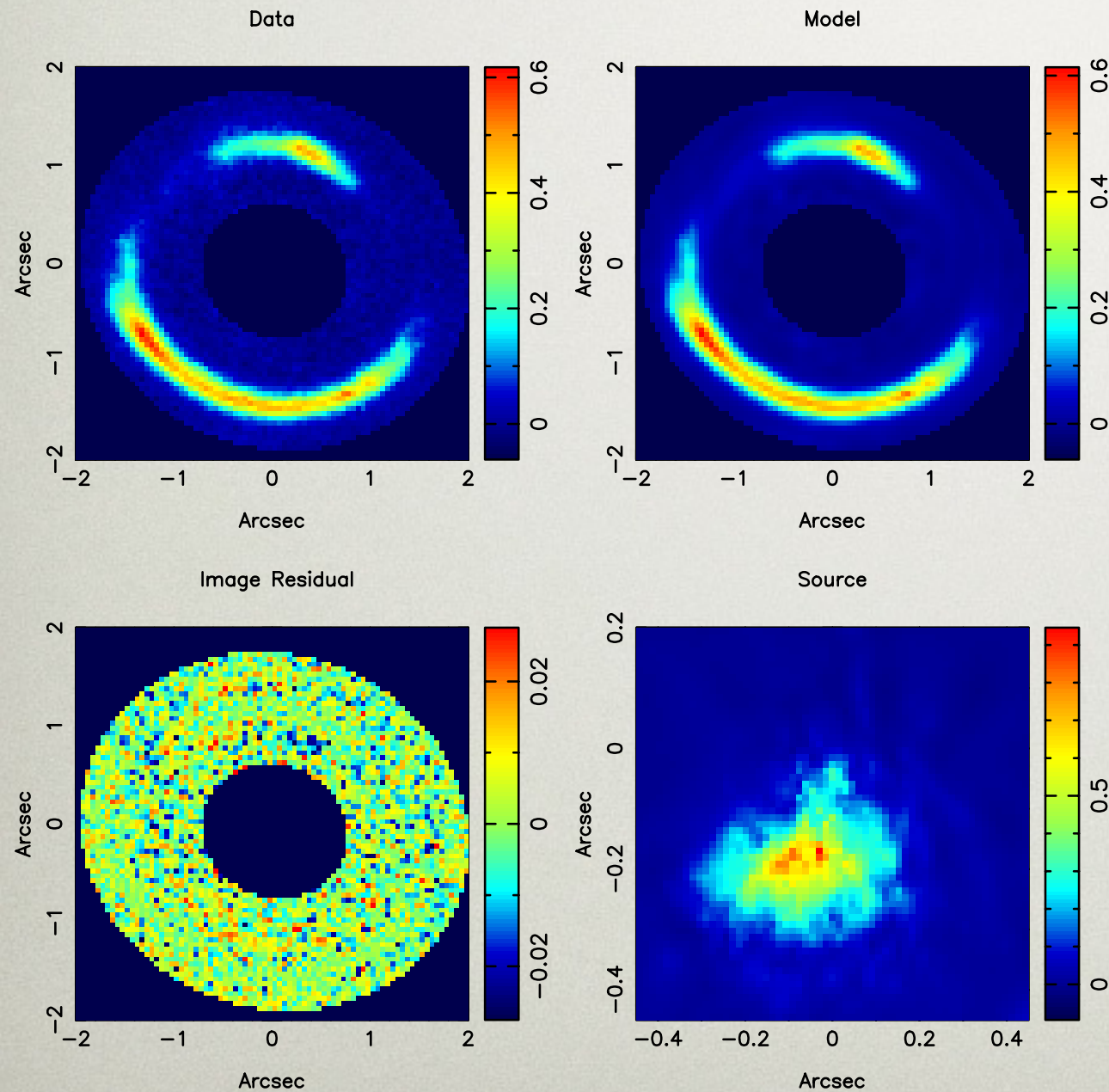
$$\mu(\alpha = 1.90, f = 0.3\%, R \in \Delta R) = 6.46 \pm 0.95$$

DOUBLE RING



— [Results are stable against changes in the PSF, lens galaxy subtraction, pixel scale and rotation

DOUBLE RING



$$M_{\text{sub}} = (3.51 \pm 0.15) \times 10^9 M_{\odot}$$

$$r_t = 1.1 \text{ kpc}$$

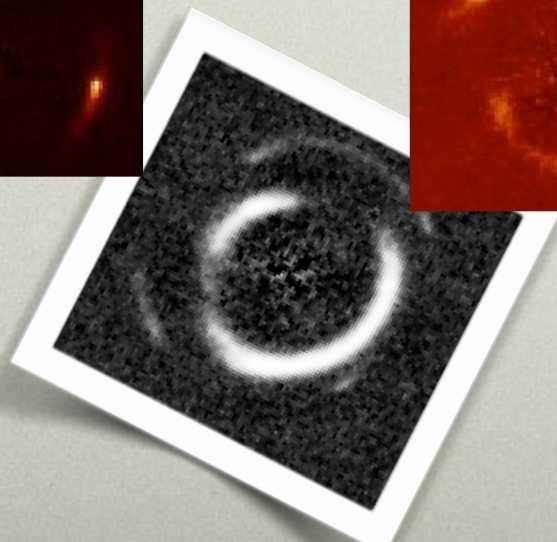
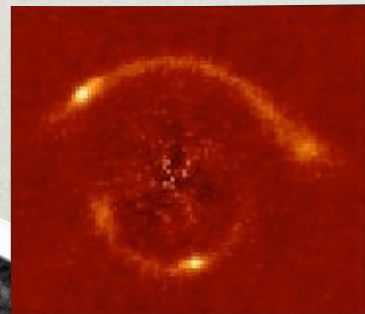
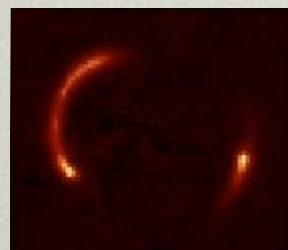
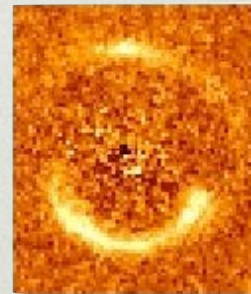
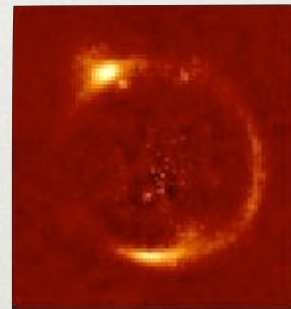
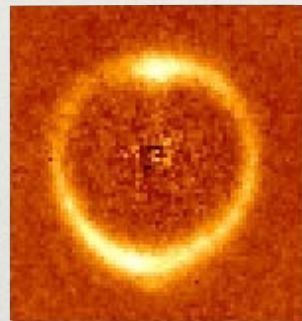
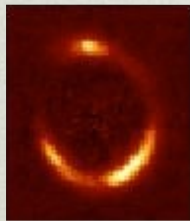
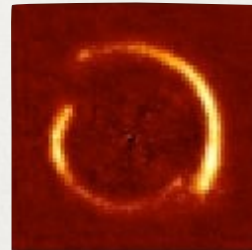
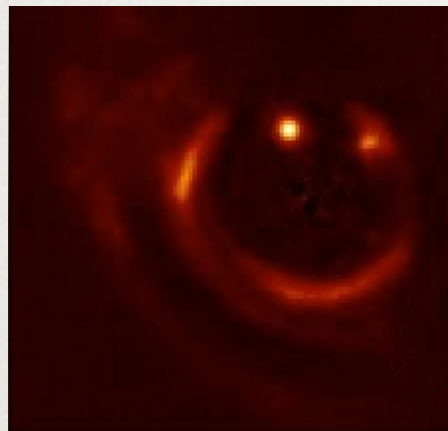
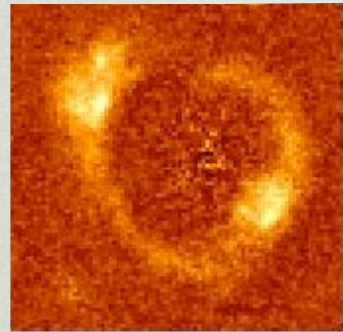
$$\Delta \log \mathcal{E} = -128.0$$

$$L_V \leq 5 \times 10^6 L_{\odot}$$

$$M_{3D}(< 0.3) = 5.83 \times 10^8 M_{\odot}$$

$$(M/L)_{V,\odot} \geq 120 M_{\odot}/L_{V,\odot}$$

$$z = 0.06 - 0.36 \quad \sigma_{\star} = 175 - 400 \text{ km s}^{-1}$$



Chosen on a s/n basis

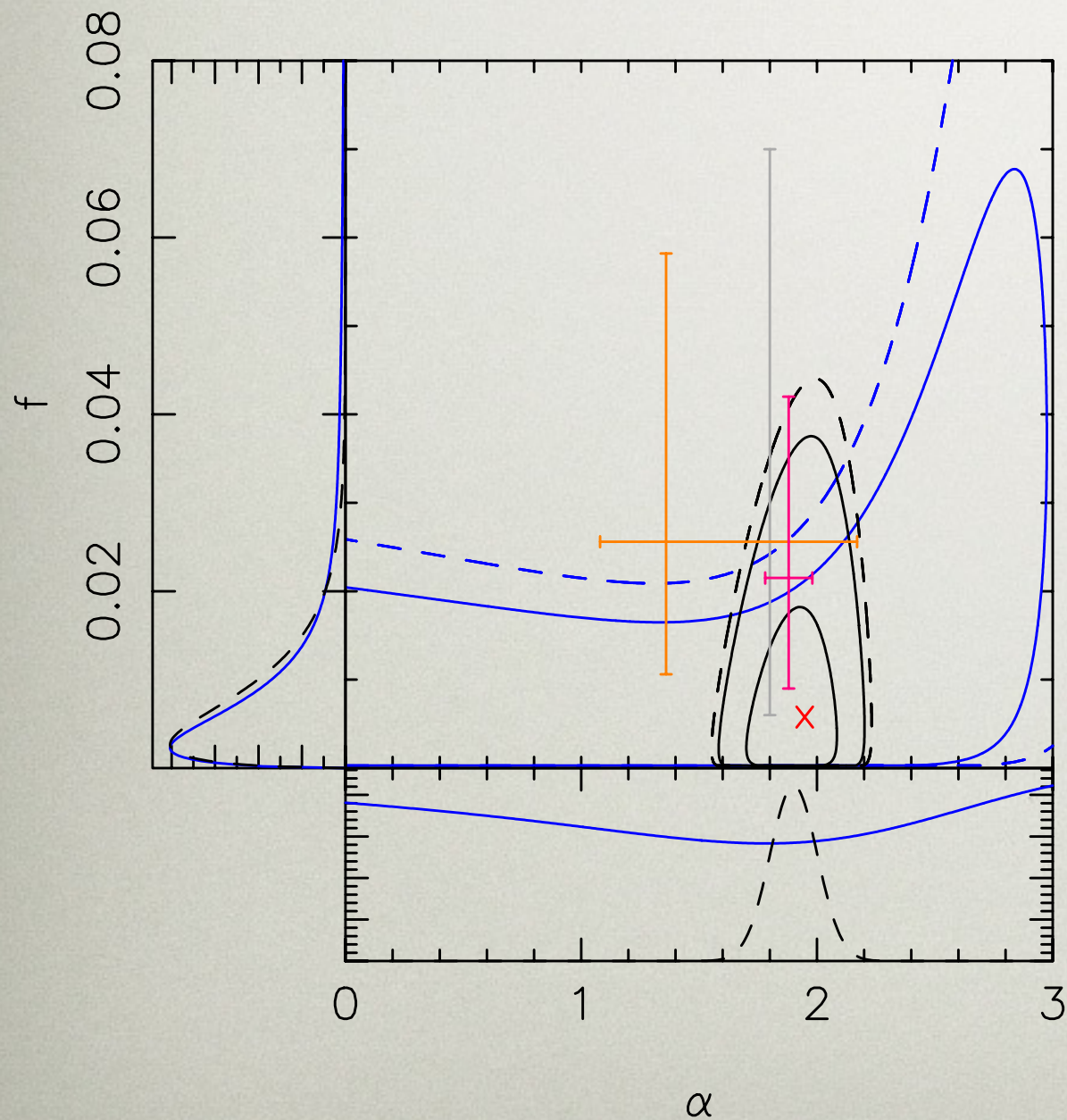


Representative sub-sample of the
SLACS lenses



Representative sample of massive
early-type galaxies

CDM MASS FUNCTION AT Z=0.2



$P(\alpha)$	f (68% CL)	α	$\ln E\nu$
U	$0.0076^{+0.0208}_{-0.0052}$	< 2.93 (95% CL)	-5.98
G	$0.0064^{+0.0080}_{-0.0042}$	$1.90^{+0.098}_{-0.098}$ (68% CL)	-6.13

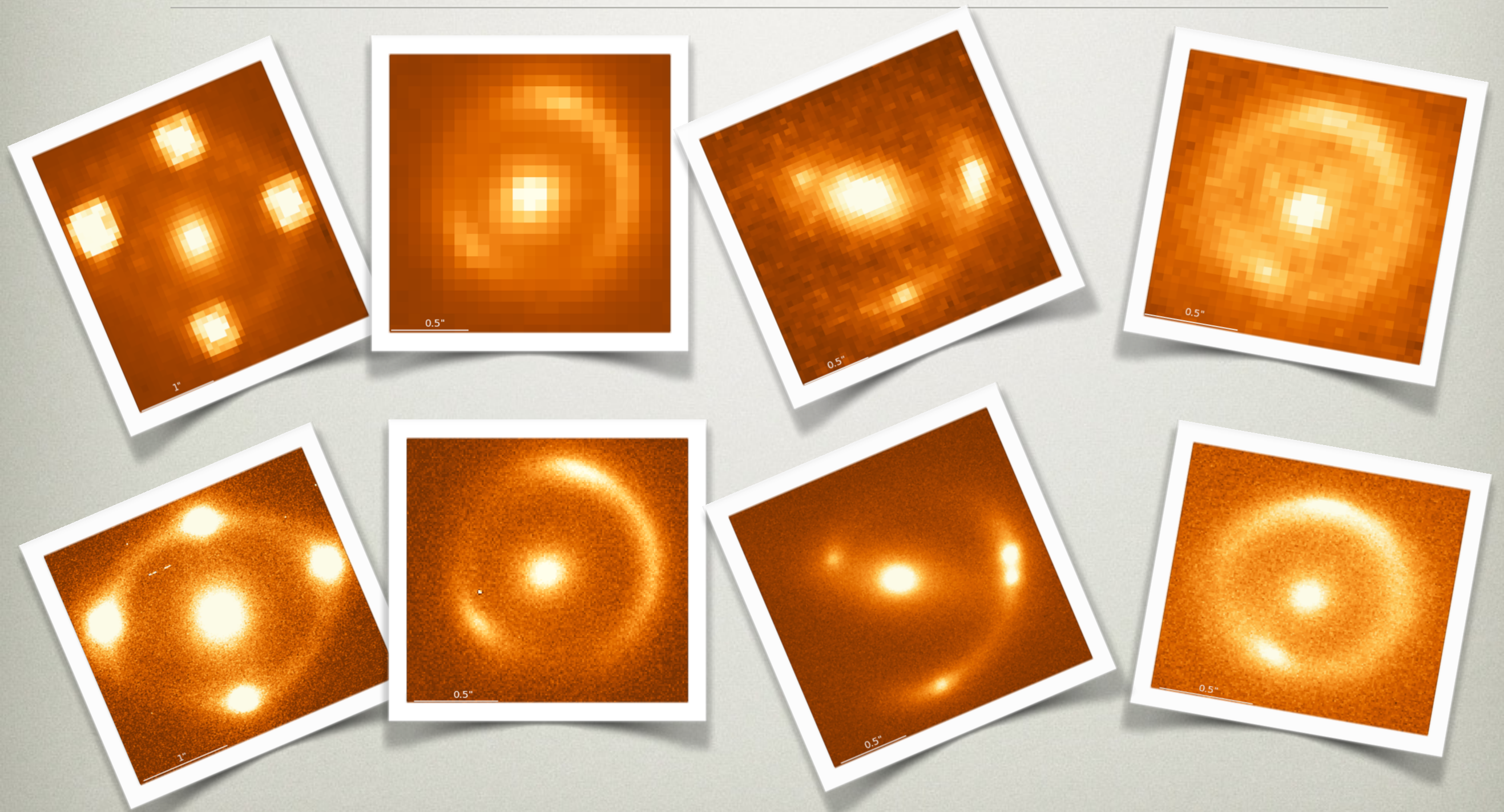
$$P(f) = \frac{1}{2(\sqrt{f_{\max}} - \sqrt{f_{\min}})\sqrt{f}}$$

$$P_U(\alpha) = \frac{1}{\alpha_{\max} - \alpha_{\min}},$$

and

$$P_G(\alpha | \mathbf{p}) = \frac{1}{\sigma_\alpha \sqrt{2\pi}} \exp\left[-\frac{(\alpha - \alpha_{\text{mean}})^2}{2\sigma_\alpha^2}\right].$$

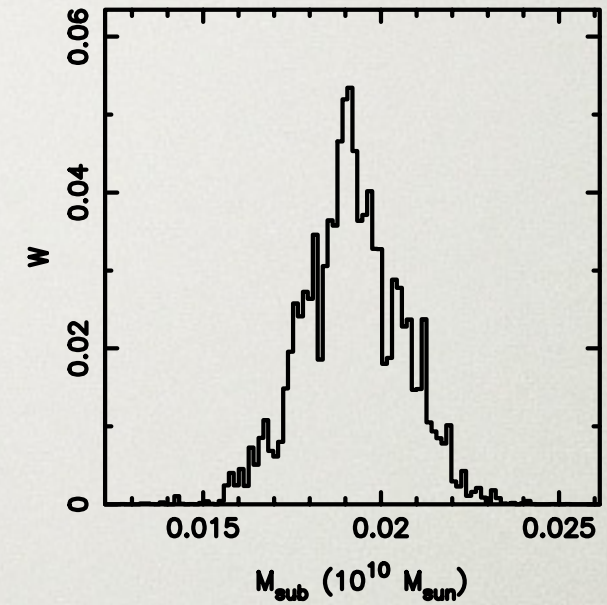
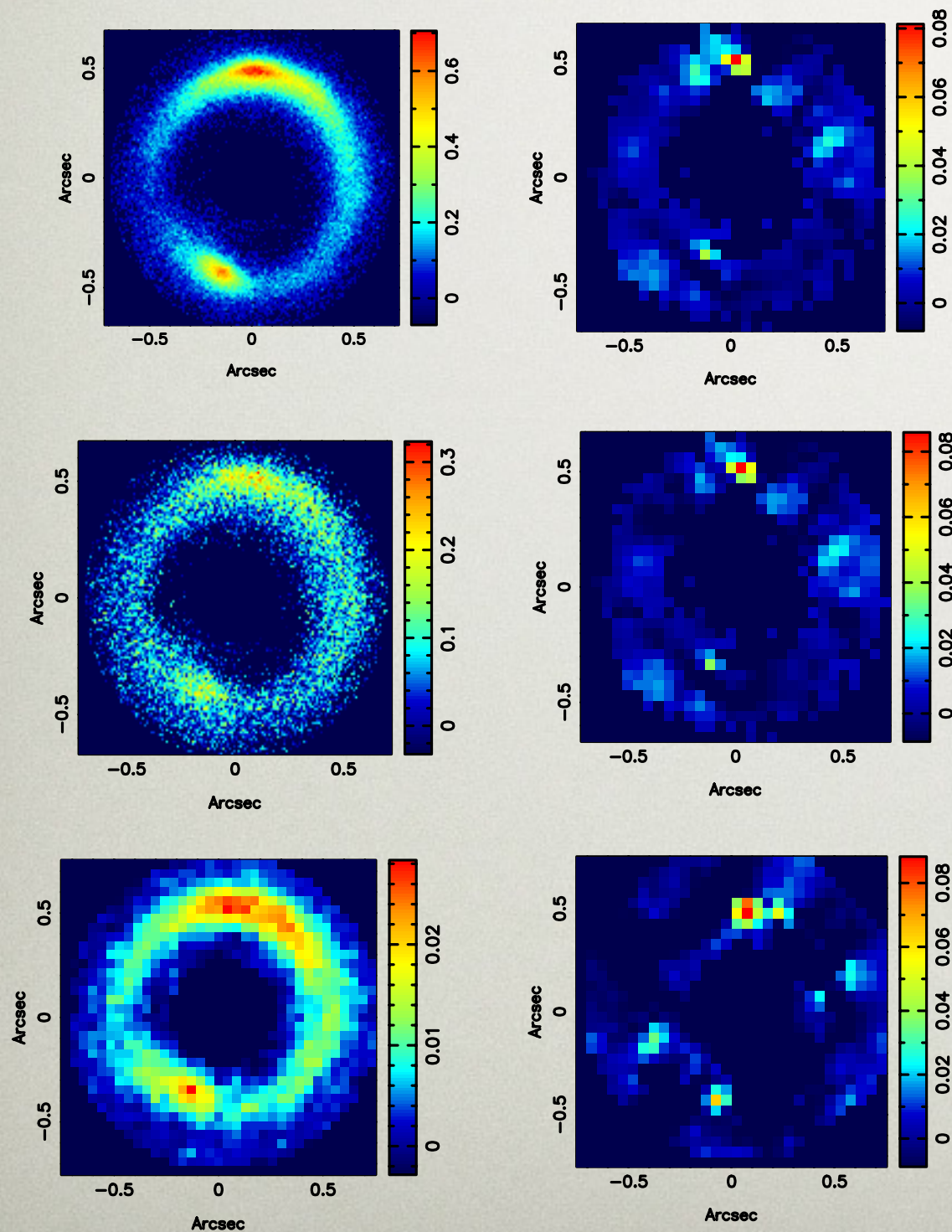
SHARP



— [Medium sized sample of ~20 systems

$$M_{low} = 10^8 M_{\odot}$$

SHARP



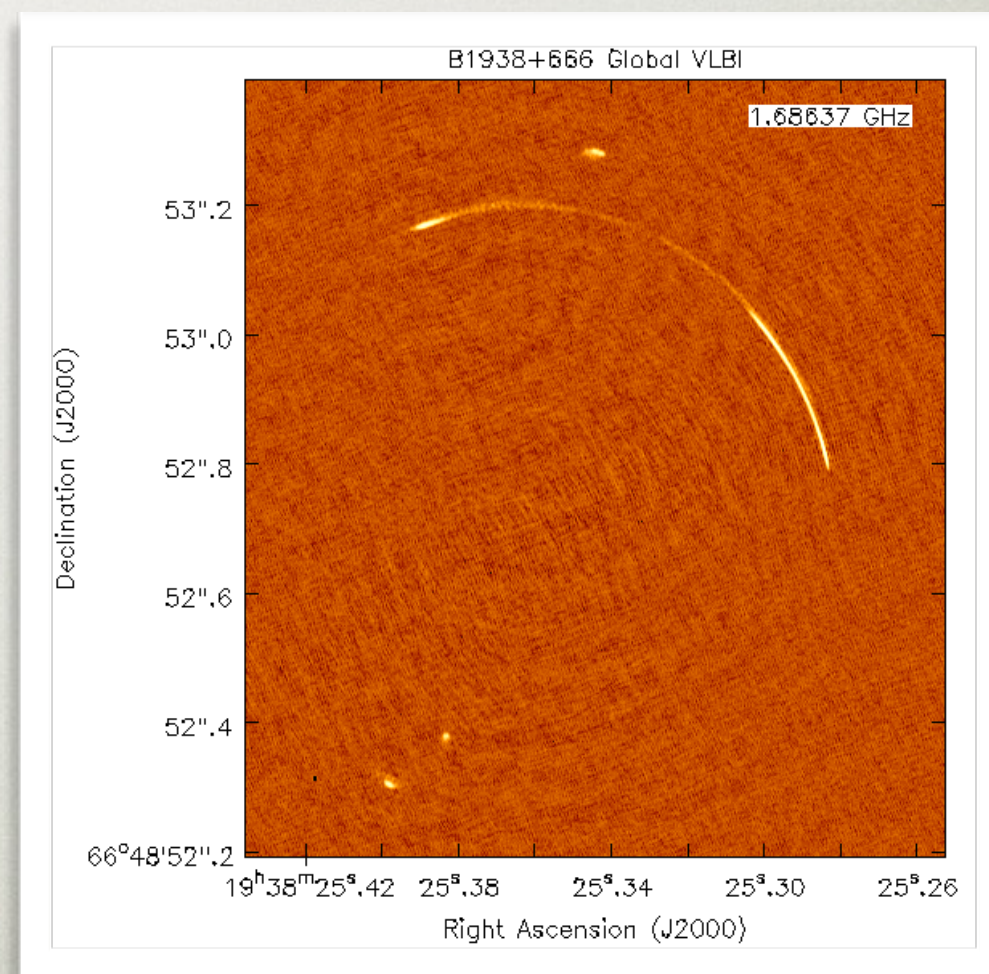
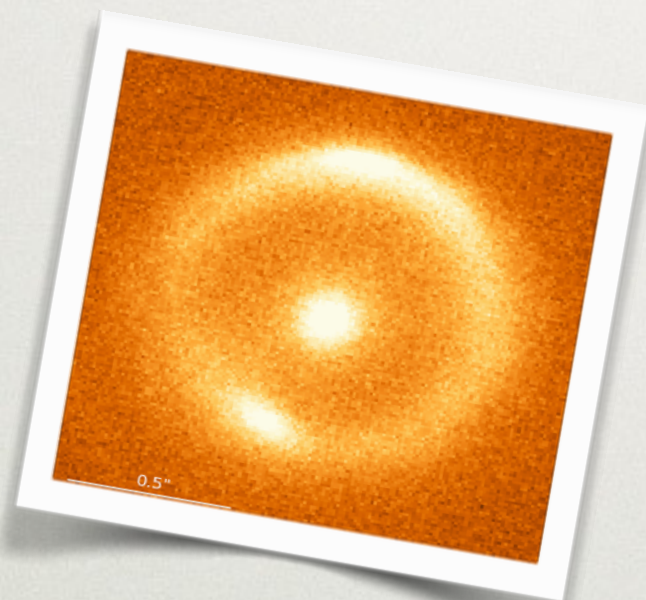
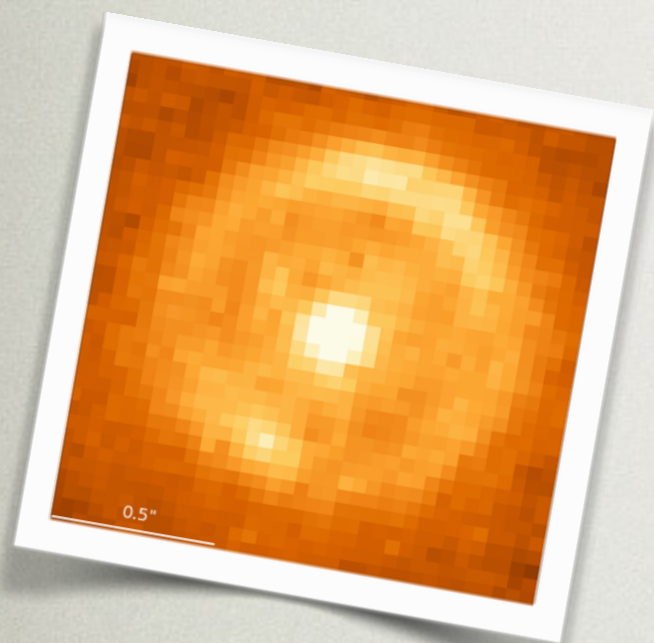
$$M_{sub} = (1.9 \pm 0.1) \times 10^8 M_{\odot}$$

$$M(< 0.6) = (1.15 \pm 0.06) \times 10^8 M_{\odot}$$

$$M(< 0.3) = (7.24 \pm 0.6) \times 10^7 M_{\odot}$$

$$V_{max} \approx 27 \text{ km s}^{-1}$$

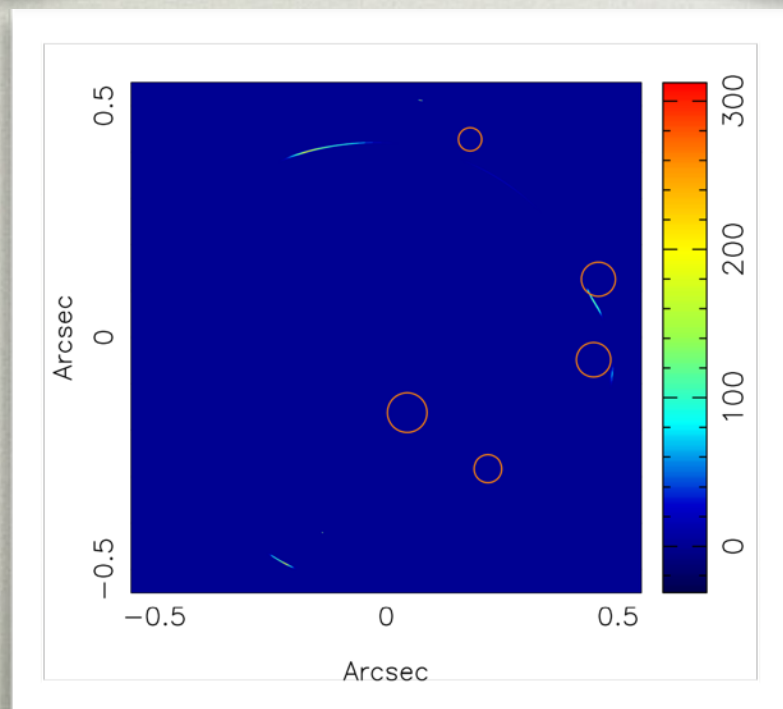
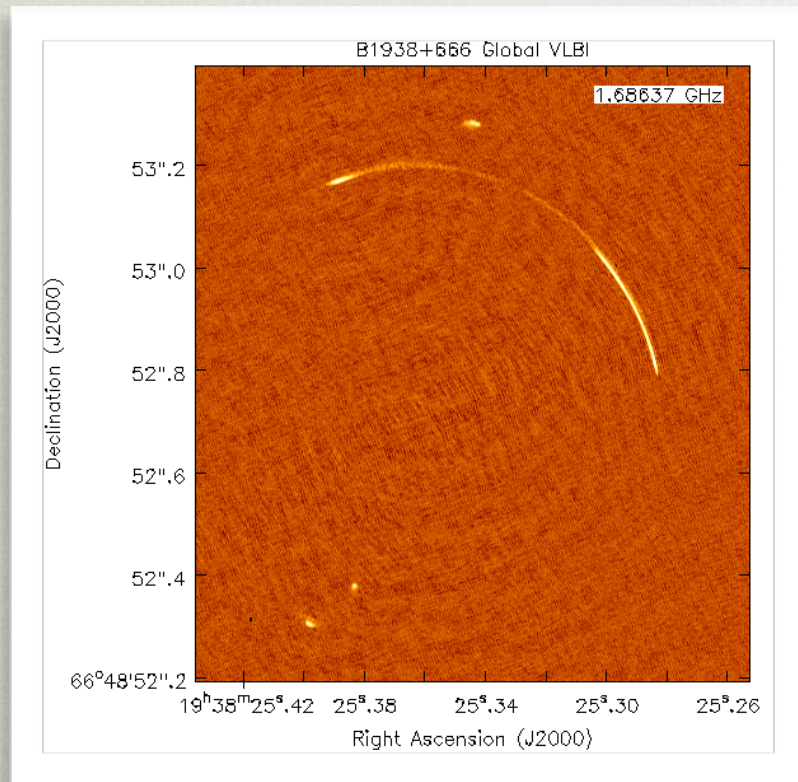
SHARP



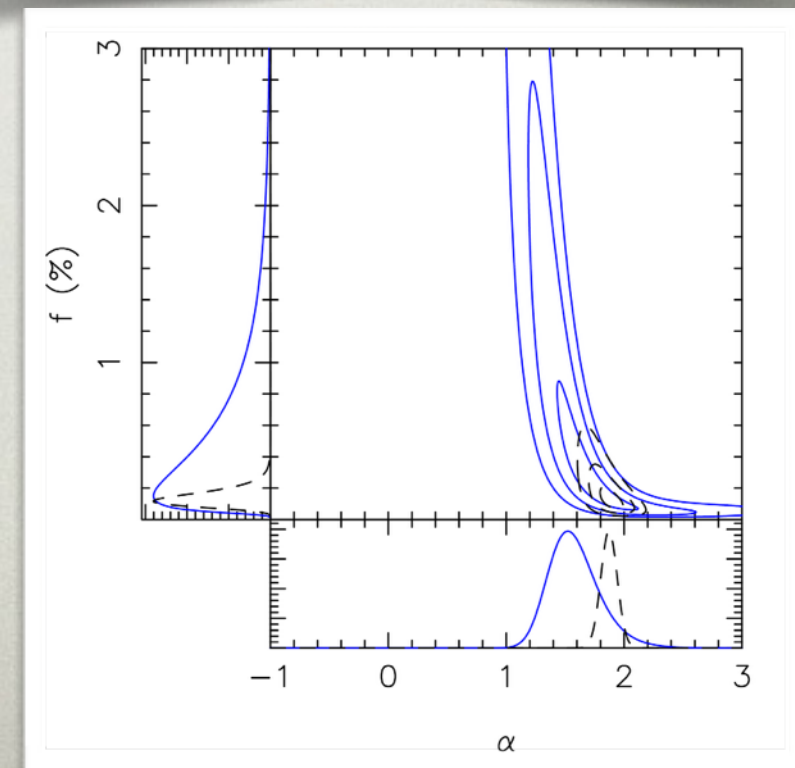
McKean et al. in prep.

Rybak et al. in prep.

RADIO - SHARP



$$f \leq 0.1\%$$



CONCLUSIONS

- [Measuring the substructure mass function is an important test of the LCDM paradigm.
- [The substructure mass function provides constraints on the dark matter properties
- [Although most of the substructure could be dark or very faint gravitational lensing provides a great tool to probe the low mass end of substructure mass function
- [Current results based on HST observations are in agreement with expectation from numerical simulation at masses $\sim 10^8 M_{\text{sun}}$